

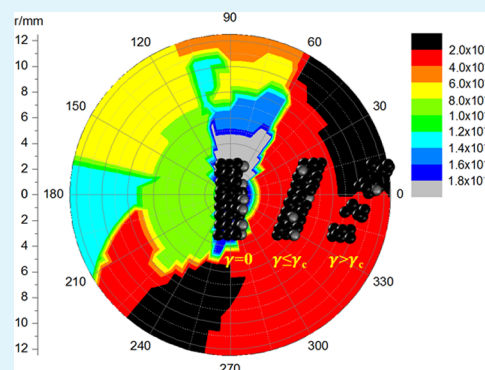
Mapping the Electrical Conductivity of Poly(methyl methacrylate)/Carbon Black Composites Prior to and after Shear

Xianhu Liu,^{†,‡} Johannes Krüchel,[†] Guoqiang Zheng,[‡] and Dirk W. Schubert^{*,†}

[†]Institute of Polymer Materials, Friedrich-Alexander-Universität Erlangen–Nuremberg, Martensstrasse 7, 91058 Erlangen, Germany

[‡]The Key Laboratory of Material Processing and Mold of Ministry of Education, College of Materials Science and Engineering, Zhengzhou University, Zhengzhou450002, China

ABSTRACT: In this letter, the electrical conductivity of disklike poly(methyl methacrylate)/carbon black composite samples was investigated prior to and after a shear process. Novel electrical conductivity maps of the samples as a function of the position were obtained. It was found that the electrical conductivity after angular averaging of the static (nonsheared) sample is, as expected, independent of the radius. However, for the sheared sample, the electrical conductivity is decreasing from the center to the outer rim of the sample. This is attributed to the interplay of destruction and buildup effects of the applied linear shear stress on the agglomerate network.



KEYWORDS: carbon black, conductivity, mapping, polymer composites, shear stress

INTRODUCTION

Conductive polymer composites (CPCs), consisting of an insulating polymer and electrical conductive fillers such as carbon black (CB) or carbon nanotubes, have been intensively studied because of their unique electrical and mechanical properties.^{1–11} Recently, there has been increasing interest in so-called coupled rheological and electrical experiments because the electrical properties of CPCs are very sensitive to the changes of the conductive structure induced by mechanical deformation.^{4–10} Furthermore, the electrical properties of CPCs depend on the size and shape of the fillers as well as their spatial distribution in the polymer matrix.^{10,11} Moreover, because of the strong intermolecular van der Waals interactions among the CB aggregates, which lead to the formation of conductive structures, it is rather difficult to disperse CB in a polymer matrix in a uniform fashion. Accordingly, it remains a question of whether there is a certain dependence of the electrical conductivity on the radial position for disklike CPC samples prior to shear and after exposure to shear. However, to our knowledge, studies on this subject are rare in the open literature, and in particular, there are no publications available on a corresponding mapping of the conductivity. In this work, disklike poly(methyl methacrylate) (PMMA)/CB composite samples were divided into several small pieces and the electrical conductivity was investigated and analyzed for each individual piece.

EXPERIMENTAL SECTION

The PMMA used as the matrix material was Plexiglas 7N from Evonik Röhm GmbH (Germany). The weight-average molar

mass and polydispersity index were 86 kg mol⁻¹ and 1.6, respectively. CB as the conductive filler was Printex XE2 from Evonik. The specific surface area was around 900 m² g⁻¹.

An internal mixer was used to prepare the composites. The conditions were as follows: 200 °C; 2 min at 20 rpm for introduction of the materials and then further 8 min at 60 rpm. Then, the samples were compression-molded to 2-mm-thick disklike plates with a diameter of 25 mm. Preheating was performed at 200 °C for 5 min with a vacuum, then hot pressing at 100 bar for 2 min, and then cooling at room temperature for 10 min. In order to prepare samples with a shear history, a stress-controlled Gemini shear rheometer (Malvern Instruments, U.K.) with a plate–plate geometry was used. The samples were annealed up to 200 °C for 15 min in order to have isothermal conditions. Then a shear step (creep test) with a constant creep stress of 20 kPa for 20 s was carried out under a nitrogen atmosphere. In order to conserve the sheared state of the conductive structures, the sheared sample was quenched to room temperature immediately after shear using a cooling spray based on tetrafluoroethane (Kontakt Chemie; Kälte 75). The samples without shear were named static samples. Prior to sample preparation and measurement, the materials were dried at 80 °C under a vacuum for at least 24 h.

A simple experimental setup was built in Erlangen and used for electrical resistance testing. In order to investigate the local

Received: July 31, 2013

Accepted: September 9, 2013

Published: September 9, 2013

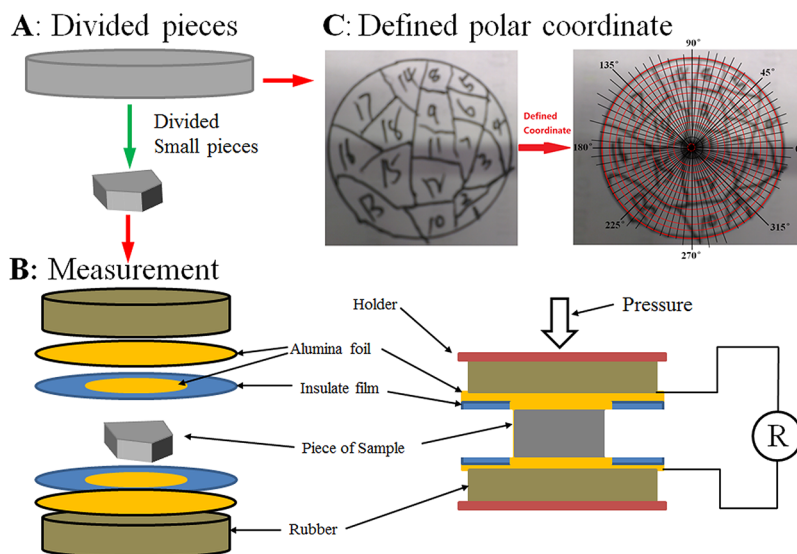


Figure 1. Schematic diagrams of the experimental and data processes.

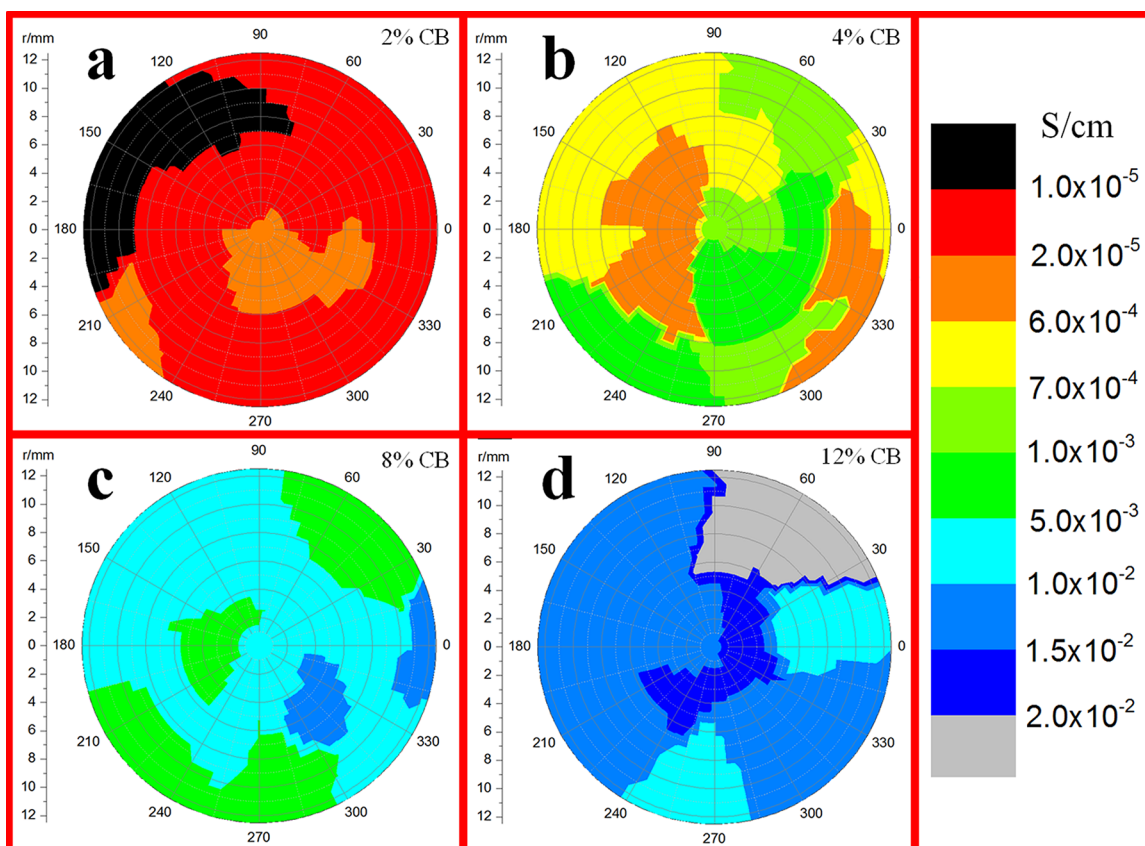


Figure 2. Electrical conductivity maps of static samples for various CB contents.

variation of the electrical conductivity of the static and sheared samples, they were divided into several small pieces (Figure 1A,C). The piece was held between two electrodes made from circular and soft alumina foil with a suitable radius. The conducting aluminum foils are at the lower and upper faces of the small pieces broken out of the sample, forming the sandwich-like geometry schematically shown in Figure 1B. Although the top and bottom surfaces of the specimens were flat, two rubbers (thickness of 3 mm) covered the aluminum foils and insulated the films to ensure a perfect composite–

electrode contact. To give an excellent conductive contact, the two aluminum foils were stuck with silver paste. The electrical resistance of each piece was measured at room temperature for a constant voltage of 1 V using a Keithley 6487 picoammeter. The electrical conductivity σ of each piece was calculated from the measured electrical resistance, R , using the following equation:

$$\sigma = \rho d^2 / Rm \quad (1)$$

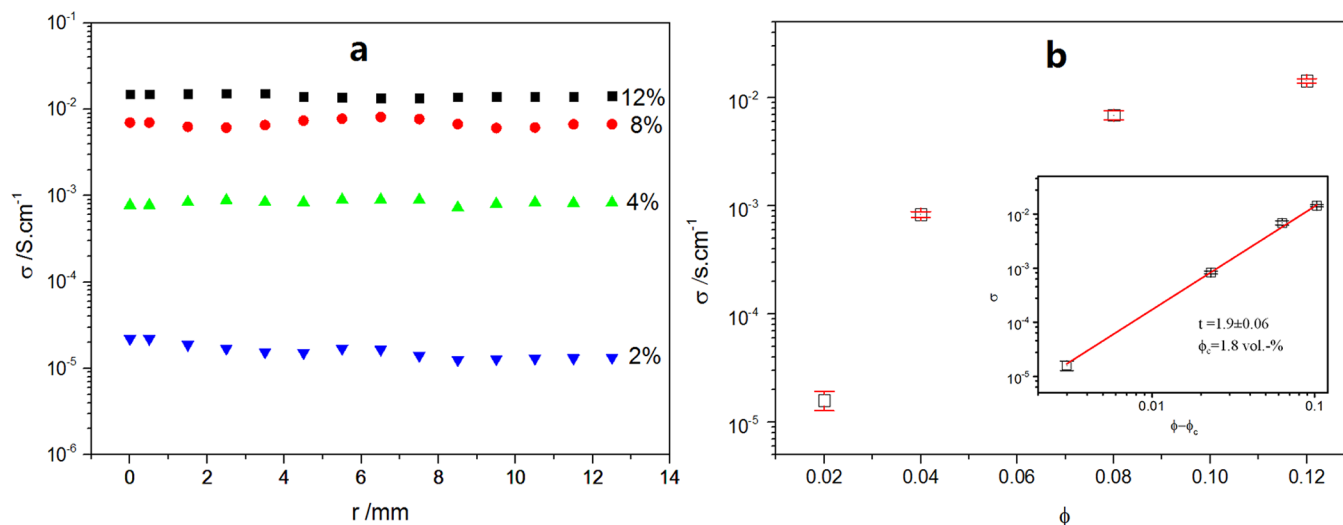


Figure 3. (a) Angular-averaged electrical conductivity of static samples for various CB contents. (b) Electrical conductivity as a function of the CB content. Inset: log–log plot of σ vs $\phi - \phi_c$.

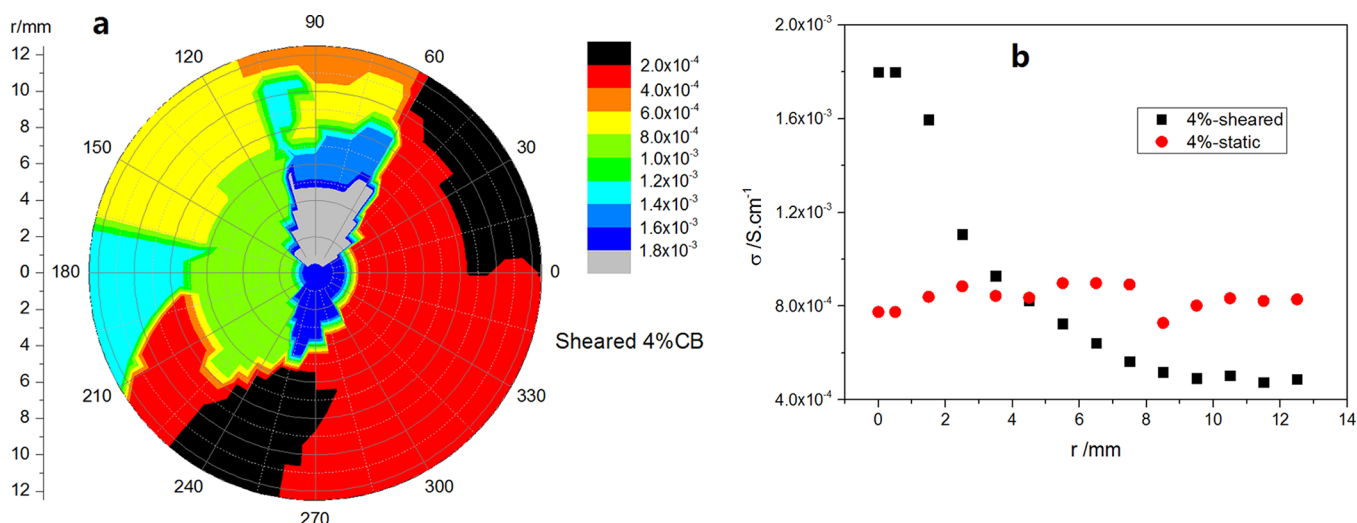


Figure 4. (a) Electrical conductivity map (units of $\text{S}\cdot\text{cm}^{-1}$) of the sheared sample. (b) Angular-averaged electrical conductivity of sheared and static samples.

where ρ , d , and m are the density, thickness, and weight of the piece, respectively. In order to obtain a conductivity map, the divided pieces were subsequently puzzled together and photographed. The resulting picture was then used to draw circles (red) and lines (black) on the map of divided pieces to define polar coordinates (Figure 1C). It was assumed that, within the small piece, the resistance is constant although, in principle, a local average over the piece.

RESULTS AND DISCUSSION

Parts a–d of Figure 2 show the electrical conductivity maps of static samples for various CB contents above the percolation threshold, set together from the individual pieces. When a polar coordinate system is applied, the electrical conductivity σ is a function of angle ϕ and radius r :

$$\sigma = \sigma(r, \phi) \quad (2)$$

Nevertheless, the electrical conductivity has to be axisymmetrical; therefore, we calculate the angular-averaged electrical conductivity:

$$\sigma(r) = \frac{\int_0^{2\pi} \sigma(r, \phi) d\phi}{2\pi} = \frac{\sum_{i=1}^N \sigma(r, \phi_i)}{N} \quad (3)$$

The sum in eq 3 holds for a discrete set of data points N evenly distributed on a circle with constant radius r . The respective results utilizing eq 3 are given in Figure 3a.

As expected, the electrical conductivity is independent of the radius (Figure 3a), and the electrical conductivity increases from $1 \times 10^{-5} \text{ S}\cdot\text{cm}^{-1}$ for 2 vol % CB to $2 \times 10^{-2} \text{ S}\cdot\text{cm}^{-1}$ for 12 vol % CB, indicating an enhancement of conductive network formation. Therefore, the mean constant electrical conductivities were plotted as a function of the CB content (Figure 3b). According to the classical percolation theory,¹² the electrical conductivity as a function of the volume fraction above the percolation threshold can be calculated using eq 4.

$$\sigma \sim (\phi - \phi_c)^t \quad (4)$$

On the basis of a known percolation threshold¹⁶ for the system of 1.8 vol %, the inset of Figure 3b clearly demonstrates that eq 4 perfectly describes the electrical conductivity as a function of

the CB content. The critical exponent t for the PMMA/CB composites is determined to be 1.9, representing a three-dimensional conductive network.

By utilizing the same procedure as that described above to a sample (4% CB content) sheared in the melt state and quenched to room temperature afterward, one obtains the map shown in Figure 4a. Similarly, one can apply the angular averaging to the sheared and quenched samples according to eq 3. From Figure 4b, it is obvious that the dependency of the electrical conductivity on the radius for the static and sheared samples presents fundamental differences.

It is well-known that the applied shear plays a significant role in the conductive pathways in CPCs.^{5–9} For the sheared sample, the electrical conductivity decreases from the center to the outer rim because of the linear increase of the deformation γ

$$\gamma = \gamma_{\max} \frac{r}{r_0} \quad (5)$$

where r_0 is the radius of the sample (12.5 mm) and γ_{\max} is the maximum deformation at r_0 , which deteriorates/destroys the conductive pathways strongest at the rim of the sheared sample. Nevertheless, it is remarkable that the sheared sample has a higher electrical conductivity in the center than the static one. However, this is probably a consequence of the additional annealing step of the sheared sample giving the system, in general, the possibility of forming more/thicker pathways that remain also under shearing in the center because there is almost a static scenario ($r = 0$). In order to explain those phenomena in more detail, a simple picture according to our work recently published is proposed (Figure 5).⁷

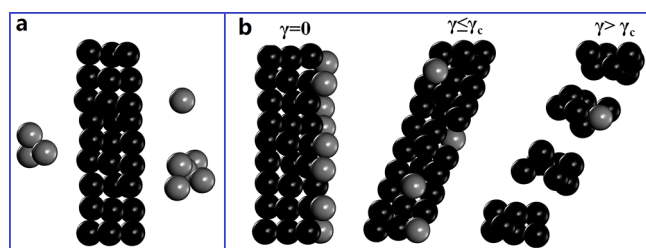


Figure 5. Schematics of the conductive CB pathway: static (a) and sheared samples with different shear states (b). CBs (gray spheres) in part a are the formation of freely separated agglomerates and/or an individual CB, which are not considered to be the formation of conductive pathways, but in part b, because of the dynamic percolation and additional annealing step allowing some free CB agglomerates to contribute to the conductive pathways, the CBs (black spheres) form the original conductive pathways.

Figure 5a shows a scenario of the conductive pathway and free CB aggregates for a static sample at room temperature. During the annealing step, the free CB aggregates become mobile and are able to connect to the existing conductive pathways because of the effect of dynamic percolation.^{6–9} Therefore, after the annealing step, the overall electrical conductivity of the sample is higher compared to the static sample, explaining the difference in the electrical conductivity at $r = 0$ in Figure 5b. While shear stress is applied, the deformation is maximal at the rim of the sample and zero in the center according to eq 5. Therefore, at deformations higher than the critical deformation $\gamma > \gamma_c$, destruction of the conductive pathways is the dominating effect in the outer

region of the sample. The existing CB pathways, which were formed by CB aggregates, will be deformed by the shear until they break into smaller agglomerates. Therefore, the electrical conductivity decreases in the outer part of the sheared sample. In the center of the sheared sample ($\gamma = 0$), no deformation takes place and the conductive pathways remain stable. In the inner part of the sample (excluding the center), although small deformation takes place for the conductive pathways ($\gamma < \gamma_c$), the thermal and flow-induced buildup of conductive pathways is the dominating effect.

CONCLUSION

In summary, the maps of the electrical conductivity for static and sheared PMMA/CB composite samples were obtained from the measured divided small pieces. The result shows that the electrical conductivity, for static samples, is independent of the radius, but for sheared samples, it decreases as the radius increases.

AUTHOR INFORMATION

Corresponding Author

*E-mail: dirk.schubert@ww.uni-erlangen.de.

Notes

The authors declare no competing financial interest.

ACKNOWLEDGMENTS

X.L. acknowledges the China Scholarship Council for funding a scholarship and Dr. Zhenxing Wang and Dr. Kun Dai for their guidance.

REFERENCES

- (1) Sherman, R. D.; Middleman, L. M.; Jacobs, S. M. *Polym. Eng. Sci.* **1983**, *23*, 36–46.
- (2) Carmona, F.; Mouney, C. *J. Mater. Sci.* **1992**, *27*, 1322–1326.
- (3) Potts, J. R.; Shankar, O.; Du, L.; Ruoff, R. S. *Macromolecules* **2012**, *45*, 6045–6055.
- (4) Kharchenko, S. B.; Douglas, J. F.; Obrzut, J.; Grulke, E. A.; Migler, K. B. *Nat. Mater.* **2004**, *3*, 564–568.
- (5) Schulz, S. C.; Schlutter, J.; Bauhofer, W. *Macromol. Mater. Eng.* **2010**, *295*, 613–617.
- (6) Krückel, J.; Starý, Z.; Triebel, C.; Schubert, D. W.; Münstedt, H. *Polymer* **2012**, *53*, 395–402.
- (7) Krückel, J.; Starý, Z.; Schubert, D. W. *Polymer* **2013**, *54*, 1106–1113.
- (8) Zhang, C.; Wang, P.; Ma, C. A.; Wu, G.; Sumita, M. *Polymer* **2006**, *47*, 466–473.
- (9) Alig, I.; Skipa, T.; Engel, M.; Lellinger, D.; Pegel, S.; Poetschke, P. *Phys. Status Solidi B* **2007**, *244*, 4223–4226.
- (10) Mamunya, Y. P.; Davydenko, V. V.; Pissis, P.; Lebedev, E. V. *Eur. Polym. J.* **2002**, *38*, 1887–1897.
- (11) Starý, Z.; Krückel, J.; Weck, C.; Schubert, D. W. *Compos. Sci. Technol.* **2013**, *85*, 58–64.
- (12) Kirkpatrick, S. *Rev. Mod. Phys.* **1973**, *45*, 574–588.